



## Two-dimensional magnetic interactions and magnetism of high-density charges in a polymer transistor

著者	Tsuji Masaki, Takahashi Yuki, Sakurai Yuki, Yomogida Yohei, Takenobu Taishi, Iwasa Yoshihiro, Marumoto Kazuhiro
journal or publication title	Applied physics letters
volume	102
number	13
page range	133301
year	2013-04
権利	(C) 2013 American Institute of Physics This article may be downloaded for personal use only. Any other use requires prior permission of the author and the American Institute of Physics. The following article appeared in Appl. Phys. Lett. 102, 133301 (2013) and may be found at <a href="http://link.aip.org/link/?apl/102/133301">http://link.aip.org/link/?apl/102/133301</a> .
URL	<a href="http://hdl.handle.net/2241/119367">http://hdl.handle.net/2241/119367</a>

## Two-dimensional magnetic interactions and magnetism of high-density charges in a polymer transistor

Masaki Tsuji, Yuki Takahashi, Yuki Sakurai, Yohei Yomogida, Taishi Takenobu et al.

Citation: *Appl. Phys. Lett.* **102**, 133301 (2013); doi: 10.1063/1.4800550

View online: <http://dx.doi.org/10.1063/1.4800550>

View Table of Contents: <http://apl.aip.org/resource/1/APPLAB/v102/i13>

Published by the [AIP Publishing LLC](#).

---

### Additional information on Appl. Phys. Lett.

Journal Homepage: <http://apl.aip.org/>

Journal Information: [http://apl.aip.org/about/about\\_the\\_journal](http://apl.aip.org/about/about_the_journal)

Top downloads: [http://apl.aip.org/features/most\\_downloaded](http://apl.aip.org/features/most_downloaded)

Information for Authors: <http://apl.aip.org/authors>

## ADVERTISEMENT

### High-Voltage Amplifiers

Voltage Range from  $\pm 50\text{V}$  to  $\pm 60\text{kV}$   
Current to 25A

### Electrostatic Voltmeters

Contacting & Non-Contacting  
Measure to 20kV - Sensitive to 1mV



ENABLING RESEARCH AND  
INNOVATION IN DIELECTRICS,  
ELECTROSTATICS, MATERIALS,  
PLASMAS AND PIEZOS



[www.trekinc.com](http://www.trekinc.com)

TREK, INC. • 11601 Maple Ridge Road, Medina, NY 14103 USA • Toll Free in USA 1-800-FOR-TREK • (t)+1-585-798-3140 • (f)+1-585-798-3106 • [sales@trekinc.com](mailto:sales@trekinc.com)

## Two-dimensional magnetic interactions and magnetism of high-density charges in a polymer transistor

Masaki Tsuji,<sup>1</sup> Yuki Takahashi,<sup>1</sup> Yuki Sakurai,<sup>1</sup> Yohei Yomogida,<sup>2</sup> Taishi Takenobu,<sup>2,3</sup> Yoshihiro Iwasa,<sup>4,5</sup> and Kazuhiro Marumoto<sup>1,3,a)</sup>

<sup>1</sup>*Division of Materials Science, University of Tsukuba, Tsukuba, Ibaraki 305-8573, Japan*

<sup>2</sup>*Department of Applied Physics, Waseda University, Tokyo 169-8555, Japan*

<sup>3</sup>*Japan Science and Technology Agency (JST), PRESTO, Kawaguchi, Saitama 322-0012, Japan*

<sup>4</sup>*Quantum-Phase Electronics Center, University of Tokyo, Tokyo 113-8656, Japan*

<sup>5</sup>*Japan Science and Technology Agency (JST), CREST, Kawaguchi, Saitama 322-0012, Japan*

(Received 21 December 2012; accepted 25 March 2013; published online 3 April 2013)

Magnetic interactions and magnetism of high-density charges in a polymer transistor were investigated by electron spin resonance (ESR). The anisotropy of the ESR spectra indicated an edge-on molecular orientation and the existence of two-dimensional magnetic interactions between the spins of the charges, reflecting high charge density. The voltage dependences revealed that the magnetism of charge carriers changed from paramagnetic to nonmagnetic as charge density increased. These results provide insight to the charge transport mechanism of polymer semiconductors with high charge densities. © 2013 American Institute of Physics. [<http://dx.doi.org/10.1063/1.4800550>]

Controlling charge density is key to tuning the physical properties of materials. Inducing high charge densities in materials by using electrolyte-gated transistor structures achieves several interesting phenomena, such as electric field-induced superconductivity<sup>1,2</sup> and electrically induced ferromagnetism at room temperature.<sup>3</sup> Moreover, electrolyte-gate technique also achieves transistor operations with high current amplification in low voltage.<sup>4–10</sup> These phenomena are due to a large amount of charge accumulation that is achieved by an electrolyte-gate dielectric in devices. The capacitances are generally very large ( $\sim 10\text{--}100\ \mu\text{F cm}^{-2}$ ), which is 100–1000 times larger than that of conventional solid-gated transistors. Interactions between charges are strong under high charge density conditions, and the electronic states differ from those at low charge densities. However, the influence of the effects cannot be sufficiently evaluated using only macroscopic characteristics, such as current-voltage characteristics. The investigation of the electronic states at a microscopic level would be extremely important not only for fundamental understanding of materials at high-charge density but also for improving the performance of electrolyte-gated transistors.

For such microscopic characterization, we have utilized electron spin resonance (ESR) as one of the microscopic characterization techniques to investigate the charge states in organic field-effect devices<sup>11–17</sup> and solar cells.<sup>18</sup> In ESR studies using field-effect devices, charges are injected into semiconductors by applying gate voltage ( $V_G$ ) that can be detected spectroscopically if the charges have magnetic moments (spins). This technique allows us to obtain microscopic properties and correlate them with macroscopic characteristics. We and other groups have investigated the various microscopic properties of organic field-effect transistors (FETs) gated by solid insulators using ESR.<sup>12,15–17,19</sup> However, electrolyte-gated transistors have not yet been studied by this ESR technique and the electronic states under high charge density were unclear.

In this letter, we report microscopic properties of polymer thin-film transistors (TFTs) such as magnetic interactions and magnetism of high-density charges using ESR; the transistors are gated by a special class of solid polymer electrolytes known as ion gels. The anisotropy of the ESR spectra indicated an edge-on molecular orientation in transistor channel and the existence of two-dimensional (2D) magnetic interactions between charges, reflecting high charge density. The voltage dependences of simultaneously evaluated ESR and FET characteristics revealed that the magnetism of the major part of charges drastically changed from paramagnetic to nonmagnetic as charge density increased. These results provide insight to the charge transport mechanism of polymer semiconductors with high charge densities.

Electrolyte-gated transistors are known to have two basic charge-induction mechanisms: electrostatic doping and electrochemical doping.<sup>4–10</sup> The two mechanisms are different from each other, but both of them can operate electrolyte-gated transistors in the low voltage region with high on/off current ratios.<sup>4–10</sup> The charge-induction mechanism of our devices is electrochemical doping. Ion gels, which consist of ionic liquids and network ABA-type triblock copolymers, are currently attracting much attention as dielectric layers because electrolyte-gated transistors based on ion gels have much better dynamic behavior than electrolyte-gated transistors based on normal solid polymer electrolytes; in addition, ion gels have more mechanical strength than ionic liquids.<sup>9,20</sup> The details of ion gels including their morphological structure are described in literatures.<sup>5,6,20–22</sup> This technology can potentially be applied in solution-processable high performance flexible electronics and in the investigation of physical properties of various materials under high charge density.

First, we explain transistor fabrication. Regioregular poly(3-hexylthiophene) (RR-P3HT) (Sigma-Aldrich) (see Fig. 1(a)) was used as the polymer semiconductor, 1-ethyl-3-methylimidazolium bis (trifluoromethylsulfonyl)imide ([EMIM][TFSI]) (Ionic Liquids Technologies) was used as

<sup>a)</sup>E-mail address: marumoto@ims.tsukuba.ac.jp

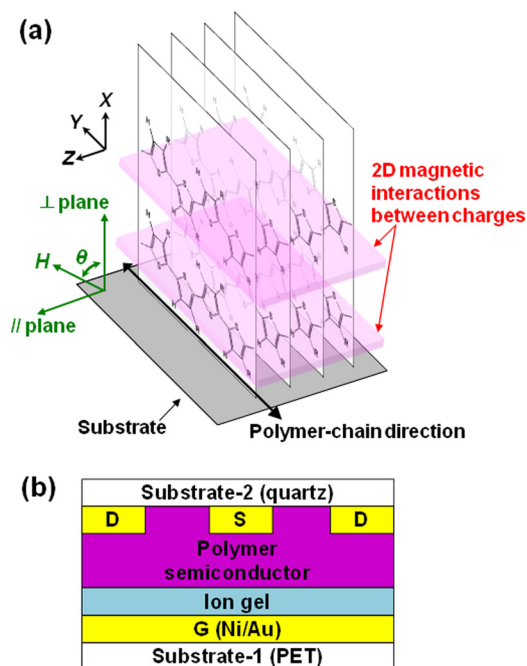


FIG. 1. (a) Schematics of the edge-on lamella structure of a film of the polymer semiconductor RR-P3HT ( $R = C_6H_{13}$ ) and 2D magnetic interactions between charges in the RR-P3HT film at high  $V_G$  regions. (b) Schematics of the TFT structure used in this study. The two drain electrodes are made to short-circuit with each other.

the ionic liquid, and poly(styrene-*b*-methylmethacrylate-*b*-styrene) (PS-PMMA-PS) (Polymer Source) was used as the ABA-type triblock copolymer. RR-P3HT is known as a high performance conducting polymer, and the combination of [EMIM][TFSI] and PS-PMMA-PS forms ion gels that shows large capacitance and high ionic conductivity.<sup>5,6,20</sup> Figure 1(b) depicts the TFT structure used in this study. Two nonmagnetic substrates of a polyethylene terephthalate (PET) film ( $30\text{ mm} \times 3\text{ mm} \times 100\text{ }\mu\text{m}$ , substrate-1) and a quartz substrate ( $30\text{ mm} \times 3\text{ mm} \times 1\text{ mm}$ , substrate-2) were used to fabricate TFTs.<sup>6,9,23</sup> Ni (3 nm)/Au (47 nm) electrodes were vapor-deposited. Ion-gel layers consisted of [EMIM][TFSI] and PS-PMMA-PS were fabricated by drop-casting on the gate electrode. The source and drain electrodes have a channel length ( $L$ ) of 0.5 mm and a total channel width ( $W$ ) of approximately 50 mm. The polymer semiconductor layers were fabricated by spin coating on the source and drain electrodes. The thickness of the films was approximately 350 nm. Finally, substrate-1 was placed on substrate-2 to complete the TFT fabrication.<sup>6,9,23</sup> All measurements were performed at room temperature in the dark and under vacuum conditions.

Next, we confirm standard transistor operation. The transfer characteristics (drain current,  $I_D$ , versus  $V_G$ ) were measured with a semiconductor device analyzer (B1500A, Agilent Technology) at a  $V_G$  sweep rate of 50 mV per 30 s and a drain voltage ( $V_D$ ) of  $-1.0\text{ V}$ . The data showed typical *p*-type transistor operation with a threshold voltage ( $V_{th}$ ) of 0.2 V, a subthreshold swing of 0.12 V/decade, an on/off current ratio larger than  $10^4$ , and a field-effect mobility ( $\mu$ ) of  $0.09\text{ cm}^2/\text{Vs}$ . These values except for  $\mu$  are approximately equivalent to those in previous reports.<sup>4-6,9</sup> The  $\mu$  was calculated from  $I_D = (W/2L)\mu C_i(V_G - V_{th})$ .<sup>2</sup> Here, the

gate-insulator capacitance per unit area  $C_i$  was estimated from  $Q_i = C_i V_G$  and  $V_D = 0\text{ V}$ . The  $Q_i$  is the accumulated charge per unit area and is calculated from the number of spins ( $N_{spin}$ ) measured with ESR. Note that the charge mobility was somewhat overestimated in this case because  $N_{spin}$  obtained from ESR measurements is lower than the number of charges owing to nonmagnetic carrier formation described below. We here comment the reason for the lower mobility of our devices compared to those in previous reports.<sup>4-6,9</sup> One possibility is due to the use of a large active area ( $L = 0.5\text{ mm}$ ,  $W = 50\text{ mm}$ ) and a thick film thickness (350 nm) compared to typically used area ( $L = 0.02\text{ mm}$ ,  $W = 0.1\text{--}0.4\text{ mm}$ ) and thickness (20 nm).<sup>5,6</sup> The reason for using such large area and thick film is to improve the signal-to-noise (SN) ratio of ESR signal, because the ESR intensity is proportional to the number of charges, which is expected to increase as the area and thickness increase owing to electrochemical transistors. The difficulty in fabricating large active area probably causes inhomogeneity of film quality, which may decrease the mobility of our devices.

Next, we show the results of ESR measurements for the TFTs. Figure 2(a) displays the ESR spectra of the TFT at  $\theta = 96^\circ$  and  $6^\circ$  at  $V_G = -0.6\text{ V}$ , and  $\theta = 6^\circ$  at  $V_G = 0.2\text{ V}$  where  $V_D = 0\text{ V}$ . Here, the abscissa  $\theta$  denotes the angle between the external magnetic field ( $H$ ) and the normal of the substrate, as shown in the inset of Figure 2(b). The ESR signal was almost absent at  $V_G = 0.2\text{ V}$  because of charge depletion. The ESR signals at  $V_G = -0.6\text{ V}$  are attributed to holes with electron spins, which have been injected into the polymer semiconductor. In other words, the origin of the ESR signal is due to positive polarons,  $P^+$ s, which have  $S = 1/2$  spins in the polymer.<sup>11,13-15</sup> The ESR measurements were performed with a JEOL JES-FA200 X-band ESR spectrometer and Keithley 2612 A source meter. The peak-to-peak ESR intensity ( $I_{ESR}$ ),  $N_{spin}$ , and  $g$ -values were calibrated by using a standard sample of a  $Mn^{2+}$  marker. The ESR linewidth ( $\Delta H_{1/2}$ ) was evaluated from the full width at half maximum of the first integrated ESR spectrum.

The angular dependence of the  $g$ -value is shown in Fig. 2(b). The anisotropy of the  $g$ -value reflects molecular orientation through anisotropic spin-orbital coupling of  $\pi$ -electrons in molecules. The anisotropy of the  $g$ -value of the RR-P3HT chains has been reported to follow the order  $g_X > g_Z > g_Y$ , where the  $Y$ -axis is parallel to the polymer chain direction, the  $Z$ -axis is perpendicular to the thiophene ring plane, and the  $X$ -axis is perpendicular to the  $Y$ - and  $Z$ -axis (see Fig. 1(a)).<sup>15</sup> The observed monotonic variation of  $g$ -value with a maximum at  $\theta = 0^\circ$  and a minimum at  $\theta = 90^\circ$  is consistent with previous ESR studies on solid insulators at low charge density.<sup>11,13-15</sup> We have also confirmed such monotonic variation of  $g$ -value at low charge density ( $V_G = -0.3\text{ V}$ ) using a similar TFT device (see Fig. 2(c)). This monotonic behavior reflects an edge-on molecular orientation of RR-P3HT due to the formation of a lamellar structure that is reported by X-ray studies as schematically shown in Fig. 1(a).<sup>11,13-15,24</sup> Note that the schematic represents the molecular orientation in a grain of RR-P3HT and also disregards the fluctuation in molecular orientation in the layer on the substrate for the sake of simplicity. In actual



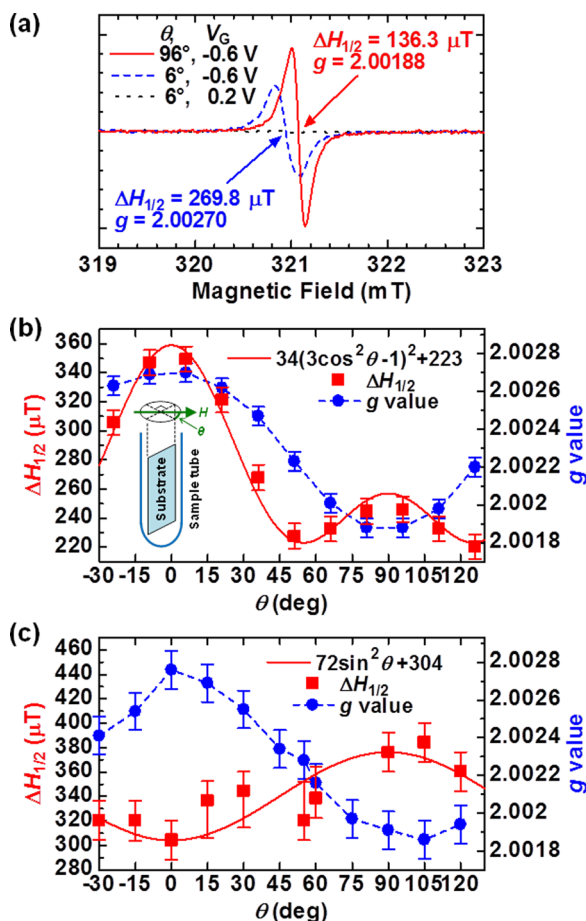


FIG. 2. (a) The ESR spectra of the TFT at  $\theta = 96^\circ$  (solid line) and  $\theta = 6^\circ$  (dashed line) at  $V_G = -0.6$  V, and  $\theta = 6^\circ$  at  $V_G = 0.2$  V where  $V_D = 0$  V. Because the ESR signal at  $V_G = 0.2$  V is almost absent, the angular dependence can be neglected. (b) Main panel: Angular dependence of the  $g$ -value (circles) and ESR linewidth  $\Delta H_{1/2}$  (squares) of the ESR signal due to polarons in the RR-P3HT at  $V_G = -0.6$  V and  $V_D = 0$  V. The solid line is a fitted curve of  $\Delta H_{1/2}$ , and the expression can be derived from the theory of exchange-narrowed ESR linewidth based on 2D magnetic dipolar interactions. Inset: Definition of the angle  $\theta$  between the external magnetic field  $H$  and the substrate. In the case of  $H$  perpendicular to the substrate,  $\theta$  is defined as  $0^\circ$ . (c) Angular dependence of the  $g$ -value (circles) and the  $\Delta H_{1/2}$  (squares) at  $V_G = -0.3$  V and  $V_D = 0$  V. The solid line is a guide to eyes.

films, the directions of the polymer chains in each grain are random due to spin coating.

In contrast to the case of the  $g$ -value, the angular dependence of the  $\Delta H_{1/2}$  at  $V_G = -0.6$  V is completely different from the monotonic variation reported in previous ESR studies. The dependence shows two maximums at  $\theta = 0^\circ$  and  $90^\circ$  and a minimum at  $\theta = 55^\circ$  (see Fig. 2(b)). In previous reports,  $\Delta H_{1/2}$  monotonically increases as  $\theta$  increases from  $0^\circ$  to  $90^\circ$ , where the origin of  $\Delta H_{1/2}$  was ascribed to hyperfine interactions between the electron spins of  $P^+$ s on carbons and the nuclear spins of hydrogen bonded to the carbons.<sup>11,13–15</sup> We have confirmed such monotonic increase in  $\Delta H_{1/2}$  at low charge density ( $V_G = -0.3$  V) (see Fig. 2(c)); large error bars are due to low SN ratio of the ESR signal. The unexpected angular dependence at  $V_G = -0.6$  V can be approximated by the expression  $\Delta H_{1/2} = A(3\cos^2\theta - 1)^2 + B$ , where  $A$  and  $B$  are constants and the  $\Delta H_{1/2}$  shows a minimum at  $\theta = 55^\circ$  (magic angle). This expression can be derived from the theory of exchange-narrowed ESR linewidth based on 2D magnetic dipolar interactions.<sup>25,26</sup> In Fig. 2(b), the solid line

shows a least-squares fit of the  $\Delta H_{1/2}$ , with fitting parameters of  $A = 34 \mu\text{T}$  and  $B = 223 \mu\text{T}$ . At higher  $V_G$  ( $-1.4$  V), we also observed the behavior  $\Delta H_{1/2} = A(3\cos^2\theta - 1)^2 + B$ , with fitting parameters of  $A = 34 \mu\text{T}$  and  $B = 681 \mu\text{T}$ . These features of  $\Delta H_{1/2}$  provide the evidence of magnetic interactions between  $P^+$ s. Such magnetic interactions had never been observed in previous ESR studies because previous devices had accumulated low-density charges. Therefore, we have discovered 2D magnetic interactions between  $P^+$ s in the RR-P3HT TFT under high charge density. These observations are schematically depicted in Fig. 1(a). The absence of interactions between layers might be due to the large distances (approximately 1.6 nm) between layers.<sup>27</sup> 2D charge transport and electronic excitations in polymer materials have been reported,<sup>24,28</sup> however, 2D magnetic interactions in polymer materials have not yet been reported.

We here discuss the reason for the change of the anisotropy in the  $g$ -value when  $V_G$  varies. At  $V_G$  below  $-0.6$  V, the anisotropy in the  $g$ -value is observed, which means that the electrolyte does not disrupt the molecular packing and change the orientation of the polymer chains. Possible explanation for observing the anisotropy is that ions of the ionic liquid penetrate into only grain boundaries in RR-P3HT films, not into grains of RR-P3HT at such low  $V_G$ . In this case, the molecular orientation of RR-P3HT is expected to be not disordered largely. On the other hand, at a high  $V_G$  ( $-1.4$  V), the anisotropy in the  $g$ -value was found to decrease considerably, which indicates the disordered molecular orientation of RR-P3HT. The reason for this disorder is probably related to the penetration of ions of the ionic liquid into RR-P3HT grains in RR-P3HT films. These penetrations will be also discussed later.

Next, we discuss the  $V_G$  and  $V_D$  dependencies of the ESR spectra. Figure 3(a) shows the dependence of  $I_{\text{ESR}}$ ,  $\Delta H_{1/2}$ , and  $N_{\text{spin}}$  on  $V_G$ . In the low  $|V_G|$  regime below  $\sim 0.8$  V,  $I_{\text{ESR}}$  and  $N_{\text{spin}}$  monotonically increased, whereas  $\Delta H_{1/2}$  was almost constant with increasing  $|V_G|$ . This behavior can be explained by the increasing number of  $P^+$ s. Here, we explain the charge induction process for this case. If the injected charges are only accumulated at the interface between the ion gel and the polymer semiconductor (electrostatic doping), approximately 18% of the thiophene rings of RR-P3HT are estimated to have been doped at a maximum  $N_{\text{spin}}$  of  $9.5 \times 10^{13}$  at  $|V_G| = 0.9$  V using lattice constants.<sup>27</sup> However, this spin concentration cannot be realized from the following reasons. First, the spatial extent of  $P^+$ s has been reported to be approximately 10 thiophene rings for regioregular poly(3-alkylthiophene).<sup>29</sup> Thus, separated  $P^+$ s cannot be formed at the estimated high spin concentration (18%), because the maximum spin concentration for the formation of separated  $P^+$ s is expected 10%. Second, in a highly doped nondegenerate conducting polymer RR-P3HT, the stable charge state has been reported to be changed from magnetic ( $S = 1/2$ ) polarons to nonmagnetic ( $S = 0$ ) polaron-pairs ( $PP^+$ s) or bipolarons ( $BP^+$ s) with increasing doping concentration or with decreasing the Coulomb interaction by theoretical and experimental studies.<sup>30,31</sup> That is, when the electron-lattice interaction or the electron-lattice coupling overcomes the electron-electron interaction,  $PP^+$ s or  $BP^+$ s is energetically stable than separated  $P^+$ s.<sup>30</sup> Thus, the estimated high spin concentration

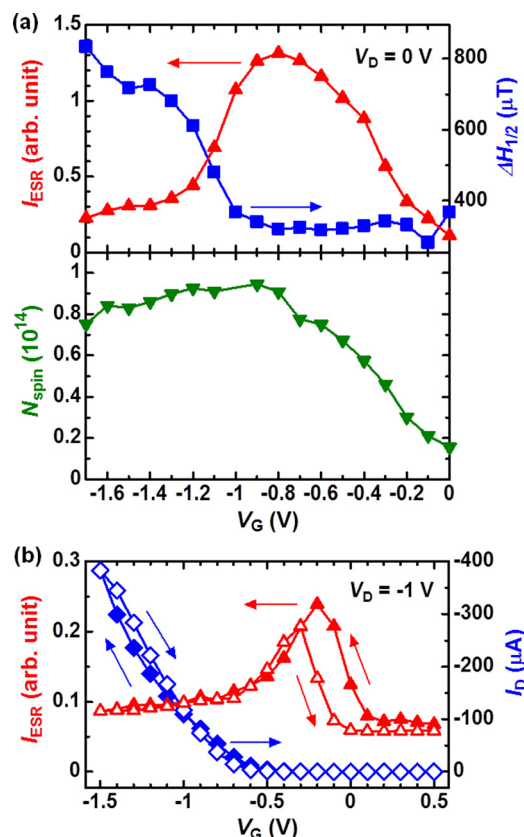


FIG. 3. (a) The dependence of the ESR intensity,  $I_{\text{ESR}}$  (up triangle),  $\Delta H_{1/2}$  (square), and number of spins,  $N_{\text{spin}}$  (down triangle) on  $V_G$ , where  $V_D = 0$  V. The  $H$  is perpendicular to the substrate. (b) The dependence of  $I_{\text{ESR}}$  (triangle) and  $I_D$  (rhombus) on  $V_G$  at  $V_D = -1.0$  V using a  $V_G$  sweep rate of 100 mV per 1440 s. The solid and open symbols represent the data for forward and reverse sweeps, respectively.

(18%) cannot be realized because of nonmagnetic charge formation mentioned above. Therefore, the charge induction process is confirmed to be electrochemical doping. Note that we obtained another evidence for electrochemical doping by measuring  $V_D$  dependence of ESR signal. The result showed that  $V_D$ -induced ESR signals were observed by applying negative  $V_D$  without  $V_G$ , whose origin is the same as that of  $V_G$ -induced ESR. The phenomena cannot be explained by the interface charge accumulation (electrostatic doping). On the other hand, if the entire polymer-semiconductor film with a thickness of  $\sim 350$  nm is assumed to be uniformly electrochemically doped, approximately 0.08% of the thiophene rings would have electron spins. However, this density is too small to observe the maximum  $N_{\text{spin}}$  because there is no maximum behavior of  $N_{\text{spin}}$  up to 0.4% doping level in the previously reported ESR studies.<sup>11,14</sup> This assumption also contradicts the existence of magnetic interactions between charges. Therefore, this result indicates a charge-density distribution in the polymer-semiconductor layer in the TFT.

To study the above charge-density distribution, we have fabricated additional devices with different RR-P3HT film thickness (approximately 90 nm) and with different device structure where source and drain electrodes were evaporated on RR-P3HT films and thus are adjacent to an ion gel. As a result, the mobility improved from 0.09 to 0.19  $\text{cm}^2/\text{Vs}$ . This result is probably explained by a gradient in charge density normal to the transistor channel, with higher charge density

near the RR-P3HT/ion-gel interface, because bulk resistance of RR-P3HT films normal to the channel in the device shown in Fig. 1(b) is larger owing to the thick film thickness (approximately 350 nm) than that of the above-mentioned additionally fabricated device.

Finally, we discuss the high-density charge region. In the high  $|V_G|$  regime above 0.9 V, a decrease in  $I_{\text{ESR}}$ , an increase in  $\Delta H_{1/2}$ , and a slight decrease in  $N_{\text{spin}}$  were observed. The feature of the  $\Delta H_{1/2}$  increase is qualitatively consistent with that by the electrochemical oxidation of RR-P3HT.<sup>31</sup> The behavior of  $N_{\text{spin}}$  can be explained by the formation of nonmagnetic charges ( $\text{PP}^{2+}$  or  $\text{BP}^{2+}$ ), as discussed above. Figure 3(b) shows the results of the simultaneous measurements of the transfer characteristics and ESR of the TFTs. While the value of  $|I_D|$  monotonically increased with increasing  $|V_G|$ , the value of  $I_{\text{ESR}}$  peaked at  $V_G$  near  $-0.2$  V and decreased for larger  $|V_G|$ . The results clearly indicate that the decrease in  $I_{\text{ESR}}$  shown in Fig. 3(a) does not indicate a decrease in accumulated charges but the formation of mobile nonmagnetic charges. The monotonic  $|I_D|$  increase implies a continuous increase in the number of hole carriers and denies the non-accumulation of hole charges. This result directly demonstrates that nonmagnetic charge transport is realized in regions with high charge density. Such nonmagnetic charge transport has not yet been reported, which is one of the physical properties caused by high-density charges. This finding indicates that the spin, which determines the paramagnetic or nonmagnetic nature of the system, can be controlled by  $V_G$ , which may be applied to produce spin transistors. Finally, we comment that organic transistors gated by electrolytes are known to have  $I_D$  maxima in transfer characteristics.<sup>4,8</sup> The relationship between the nonmagnetic charge states clarified from this study and the  $I_D$  maxima is an interrelated problem and is open for future studies.

In summary, we have fabricated ion gel-gated polymer TFTs with RR-P3HT as the polymer semiconductor, [EMIM][TFSI] as the ionic liquid, and PS-PMMA-PS as a triblock copolymer; we then studied them by ESR. From the anisotropy of the  $g$ -value, the molecular orientation of the RR-P3HT layer was confirmed to be edge-on. Moreover, from the anisotropy of  $\Delta H_{1/2}$ , we discovered 2D magnetic interactions between holes caused by high charge densities. The simultaneous measurements of the ESR and transfer characteristics clarified that nonmagnetic hole transport ( $\text{PP}^{2+}$  or  $\text{BP}^{2+}$ ) occurs at high charge densities. From this study, we propose that magnetic interactions between charges and magnetism need to be considered to understand the charge transport mechanism at high charge densities; these interactions also need to be considered when studying the potential of spin engineering or field-induced superconductivity in conducting polymers.

We thank Y. Shimoi, H. Shimotani, and D. Son for their fruitful discussions. This work was partly supported by Grants-in-Aid for Scientific Research (24560004 and 22340080) from the Japan Society for the Promotion of Science (JSPS) and by JST, PRESTO. Y.I. was supported by Grant-in-Aid for Scientific Research (21224009), "Funding Program for World-Leading Innovative R&D on Science and Technology (FIRST Program)" from JSPS, and the Strategic International Collaborative Research Program (SICORP) from JST.

- <sup>1</sup>K. Ueno, S. Nakamura, H. Shimotani, A. Ohtomo, N. Kimura, T. Nojima, H. Aoki, Y. Iwasa, and M. Kawasaki, *Nature Mater.* **7**, 855 (2008).
- <sup>2</sup>J. T. Ye, S. Inoue, K. Kobayashi, Y. Kasahara, H. T. Yuan, H. Shimotani, and Y. Iwasa, *Nature Mater.* **9**, 125 (2010).
- <sup>3</sup>Y. Yamada, K. Ueno, T. Fukumura, H. T. Yuan, H. Shimotani, Y. Iwasa, L. Gu, S. Tsukimoto, Y. Ikuhara, and M. Kawasaki, *Science* **332**, 1065 (2011).
- <sup>4</sup>M. J. Panzer and C. D. Frisbie, *J. Am. Chem. Soc.* **129**, 6599 (2007).
- <sup>5</sup>J. H. Cho, J. Lee, Y. Xia, B. Kim, Y. He, M. J. Renn, T. P. Lodge, and C. D. Frisbie, *Nature Mater.* **7**, 900 (2008).
- <sup>6</sup>J. Lee, L. G. Kaake, J. H. Cho, X.-Y. Zhu, T. P. Lodge, and C. D. Frisbie, *J. Phys. Chem. C* **113**, 8972 (2009).
- <sup>7</sup>J. D. Yuen, A. S. Dhoot, E. B. Namdas, N. E. Coates, M. Heeney, I. McCulloch, D. Moses, and A. J. Heeger, *J. Am. Chem. Soc.* **129**, 14367 (2007).
- <sup>8</sup>M. J. Panzer and C. D. Frisbie, *Adv. Mater.* **20**, 3177 (2008).
- <sup>9</sup>J. H. Cho, J. Lee, Y. He, B. S. Kim, T. P. Lodge, and C. D. Frisbie, *Adv. Mater.* **20**, 686 (2008).
- <sup>10</sup>Y. Yomogida, J. Pu, H. Shimotani, S. Ono, S. Hotta, Y. Iwasa, and T. Takenobu, *Adv. Mater.* **24**, 4392 (2012).
- <sup>11</sup>K. Marumoto, Y. Muramatsu, Y. Nagano, T. Iwata, S. Ukai, H. Ito, S. Kuroda, Y. Shimoi, and S. Abe, *J. Phys. Soc. Jpn.* **74**, 3066 (2005).
- <sup>12</sup>K. Marumoto, S. Kuroda, T. Takenobu, and Y. Iwasa, *Phys. Rev. Lett.* **97**, 256603 (2006).
- <sup>13</sup>S. Watanabe, K. Ito, H. Tanaka, H. Ito, K. Marumoto, and S. Kuroda, *Jpn. J. Appl. Phys., Part 2* **46**, L792 (2007).
- <sup>14</sup>S. Kuroda, S. Watanabe, K. Ito, H. Tanaka, H. Ito, and K. Marumoto, *Appl. Magn. Reson.* **36**, 357 (2009).
- <sup>15</sup>S. Watanabe, H. Tanaka, S. Kuroda, A. Toda, S. Nagano, T. Seki, A. Kimoto, and J. Abe, *Appl. Phys. Lett.* **96**, 173302 (2010).
- <sup>16</sup>K. Marumoto, N. Arai, H. Goto, M. Kijima, K. Murakami, Y. Tominari, J. Takeya, Y. Shimoi, H. Tanaka, S. Kuroda, T. Kaji, T. Nishikawa, T. Takenobu, and Y. Iwasa, *Phys. Rev. B* **83**, 075302 (2011).
- <sup>17</sup>M. Tsuji, N. Arai, K. Marumoto, J. Takeya, Y. Shimoi, H. Tanaka, S. Kuroda, T. Takenobu, and Y. Iwasa, *Appl. Phys. Express* **4**, 085702 (2011).
- <sup>18</sup>K. Marumoto, T. Fujimori, M. Ito, and T. Mori, *Adv. Energy Mater.* **2**, 591 (2012).
- <sup>19</sup>H. Matsui, T. Hasegawa, Y. Tokura, M. Hiraoka, and T. Yamada, *Phys. Rev. Lett.* **100**, 126601 (2008).
- <sup>20</sup>K. H. Lee, S. Zhang, T. P. Lodge, and C. D. Frisbie, *J. Phys. Chem. B* **115**, 3315 (2011).
- <sup>21</sup>M. A. B. H. Susan, T. Kaneko, A. Noda, and M. Watanabe, *J. Am. Chem. Soc.* **127**, 4976 (2005).
- <sup>22</sup>S. Imaizumi, H. Kokubo, and M. Watanabe, *Macromolecules* **45**, 401 (2012).
- <sup>23</sup>A. Kösemen, S. E. San, M. Okutan, Z. Doğruyol, A. Demir, Y. Yerli, B. Şengez, E. Başaran, and F. Yılmaz, *Microelectron. Eng.* **88**, 17 (2011).
- <sup>24</sup>H. Sirringhaus, P. J. Brown, R. H. Friend, M. M. Nielsen, K. Bechgaard, B. M. W. Langeveld-Voss, A. J. H. Spiering, R. A. J. Janssen, E. W. Meijer, P. Herwig, and D. M. de Leeuw, *Nature* **401**, 685 (1999).
- <sup>25</sup>M. Pomerantz, F. H. Dacol, and A. Segmüller, *Phys. Rev. Lett.* **40**, 246 (1978).
- <sup>26</sup>S. Kuroda, K. Marumoto, H. Kihara, H. Ofuchi, M. Tabuchi, Y. Takeda, A. G. Banskchikov, N. S. Sokolov, and N. L. Yakovlev, *Jpn. J. Appl. Phys., Part 2* **40**, L1151 (2001).
- <sup>27</sup>S. Joshi, S. Grigorian, and U. Pietsch, *Phys. Status Solidi A* **205**, 488 (2008).
- <sup>28</sup>R. Österbacka, C. P. An, X. M. Jiang, and Z. V. Vardeny, *Science* **287**, 839 (2000).
- <sup>29</sup>K. Marumoto, N. Takeuchi, and S. Kuroda, *Chem. Phys. Lett.* **382**, 541 (2003).
- <sup>30</sup>Y. Shimoi, M. Kuwabara, and S. Abe, *Synth. Met.* **119**, 213 (2001).
- <sup>31</sup>X. Jiang, R. Patil, Y. Harima, J. Ohshita, and A. Kunai, *J. Phys. Chem. B* **109**, 221 (2005).